

**Nanoconjugates of graphene oxide derivatives and meso-tetraphenylporphyrin: A new
avenue for anticancer photodynamic therapies - *Cell-on-a-Chip* analysis**

*A. Zuchowska, A. Kasprzak, B. Dabrowski, K. Kaminska, M. Poplawska, Z. Brzozka**

New Journal of Chemistry

Supplementary Information

Table of contents

S1.	Materials and methods	2
S2.	Synthesis and characterization of GO-based materials	3
S3.	FT-IR spectra, RAMAN spectra, TGA curves and elemental analysis	6
S4.	Microbiological purity of GO	15
S5.	Fabrication of the microsystem.....	15
S6.	Photodynamic effect of GO_TPP <i>in vitro</i>	16
References.....		17

S1. Materials and methods

The sonication was performed using a Bandelin Sonorex RK 100 H ultrasonic probe with a temperature control (ultrasonic peak output/HF power: 320W/80W; 35 kHz). The suspensions of GO materials were centrifuged in a MPW-260R centrifuge with a temperature control.

Fourier-transform infrared (FT-IR) spectra were recorded in a transmission mode with the Thermo Nicolet Avatar 370 spectrometer with spectral resolution of 4 cm⁻¹. The samples were mixed with KBr and pressed in a form of pellets.

FT-Raman spectra were recorded on a Bruker IFS66 instrument equipped with a FRA 106 FT-Raman module and a Nd:YAG laser (1064 nm) as a laser source.

Thermogravimetric analyses (TGA) were performed with a Netzsch STA449C thermobalance under argon atmosphere with a heating rate of 10 °Cmin⁻¹.

Elemental analyses were performed using CHNS Elementar Vario EL III apparatus. Each elemental composition was reported as an average of two analyses.

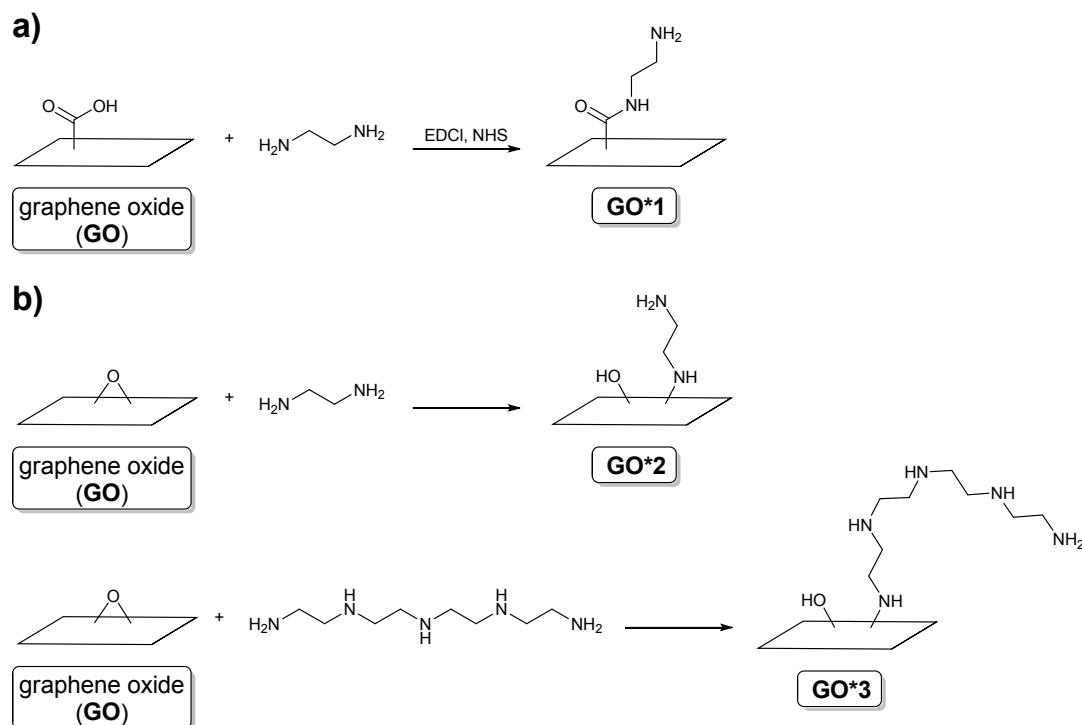
The microbiological purity of the graphene oxide (GO) suspension was evaluated. For this purpose, the surface spread method was used. The inoculation of GO suspension was carried out on Sabouraud substrate (for fungal) and Mueller-Hinton agar (MHA) (for bacteria) and incubated 48 h at 36°C. After this time, the presence of fungal and bacteria colonies were evaluated.

S2. Synthesis and characterization of GO-based materials

Synthesis design

Functionalization of GO: synthesis and characterization

Two methods for the amino-functionalization of graphene oxide (GO) were developed. The first synthetic path (**Scheme S1a**) was based on the carbodiimide-mediated amidation-type reaction between carboxylic functionalities of GO and primary amino groups of ethylenediamine (material **GO*1** was obtained). The second functionalization method (**Scheme S1b**) involved the epoxide opening-driven treatment of GO with an excess of diamine (ethylenediamine or tetraethylenepentamine used, material **GO*2** or **GO*3** was obtained, respectively). The excess of diamines were used in order to exclude self-conjugation between graphene sheets. The obtained materials were characterized in detail with various techniques, i.e., Fourier-transform infrared spectroscopy (FT-IR), Raman spectroscopy, thermogravimetric analysis (TGA) and elemental analysis.



Scheme S1. Synthesis of amino derivatives of GO: **(a)** amidation-type reaction, **(b)** epoxide opening reaction.

FT-IR spectra of the obtained materials (**Fig. S1**) featured the absorption bands coming from the graphene sheet and from the introduced moieties. In the spectra of each functionalized material (**GO*1**, **GO*2** and **GO*3**) the strong absorption band located at 1580 cm^{-1} was ascribed to the N-H stretching vibrations coming from the primary amino groups. Thus, this feature confirmed the successful introduction of the NH_2 moieties onto the GO surface. In the spectrum of material **GO*1**, the strong absorption band located at 1650 cm^{-1} was ascribed to the C=O stretching vibrations coming from presence of the amide functionality in the sample. Additionally, in the spectrum of each functionalized material, the strong absorption band located at 1720 cm^{-1} , coming from the C=O stretching vibrations of GO's carboxylic groups, was not observed. For the **GO*1** it was a result of formation of the amide-type linkages. For the **GO*2** and **GO*3** this feature was associated with the presence of the NH_2 groups on the material's surface, which resulted in the shift of the C=O band to lower wavelengths due to a $\text{COOH} \leftrightarrow \text{NH}_2$ hydrogen-bonding interactions.

Raman spectroscopy was applied to further confirm the successful functionalization of GO. The direct comparison between the Raman spectra (**Fig. S6**) of native GO and **GO*1**, **GO*2** and **GO*3** brings a conclusion that the samples of the functionalized GO are characterized by the higher degree of degradation than the native GO (a change in I_D/I_G ratio). It is noteworthy that samples **GO*2** and **GO*3** contain more defected sites in GO's sheet than **GO*1** (please compare the relative I_D intensities located at 1345 cm^{-1}). This feature is related to the applied functionalization route: epoxide opening reaction (**GO*2** and **GO*3**) influenced on the lower level of graphitization than the amidation-type process with the inclusion of GO's carboxylic functionalities (**GO*1**).

TGA curves for the functionalized GO materials and for the native GO are presented in **Fig. 11**. Weight loss up to ca. 120°C was ascribed to the presence of moisture in the sample, whilst the further weight loss was a result of thermal decomposition of organic functionalities. Different

TGA profile and higher weight loss up to 700°C in the TGA curves for **GO*1**, **GO*2** and **GO*3** in comparison to native GO were attributed to the presence of the introduced organic moieties onto the graphene sheet.

Finally, elemental analysis confirmed the presence of the amino functionalities in the samples of the functionalized GO materials (**Table S1**). Native GO did not contain nitrogen, whilst the composition of **GO*1**, **GO*2** and **GO*3** included 9-15 at% of nitrogen.

Characterization of conjugates of tetraphenylporphyrin (TPP) and GO-based materials

FT-IR spectroscopy confirmed the presence of the adsorbed TPP on the surface of GO materials (**Figs. S2-S5**). The spectra of each material containing TPP were similar and featured the strong absorption bands clearly coming from TPP, such as at ca. 1470, 1365, 960, 800 and 700 cm⁻¹.^[4] Raman spectroscopy provided further spectroscopic confirmation for the success of anchoring TPP onto the graphene sheet of **GO**, **GO*1**, **GO*2** and **GO*3** (**Figs. S7-S10**). A difference in the I_D/I_G ratio after the reaction with TPP supported our thesis on the introduction of TPP to the graphene material.

TGA profiles for the GO-based materials with anchored TPP were different than the ones for the respective starting materials (**GO**, **GO*1**, **GO*2** or **GO*3**; **Figs. S12-S15**).

In general, the TGA curve profile between 200-550 °C was similar for all the samples containing TPP, featuring a relative plateau segment between 200-450 °C followed by the significant, fast weight loss between 450-520 °C. Additionally, a weight loss up to 700°C was found to be different between the respective samples. These features were clearly ascribed to the presence of TPP onto the material.

The C:H:N ratio obtained from the elemental analysis for the **GO_TPP**, **GO*1_TPP**, **GO*2_TPP** and **GO*3_TPP** was different in comparison to the respective GO materials (**GO**, **GO*1**, **GO*2** and **GO*3**; see data in Table S1). This difference resulted from the presence of the adsorbed TPP.

S3. FT-IR spectra, RAMAN spectra, TGA curves and elemental analysis

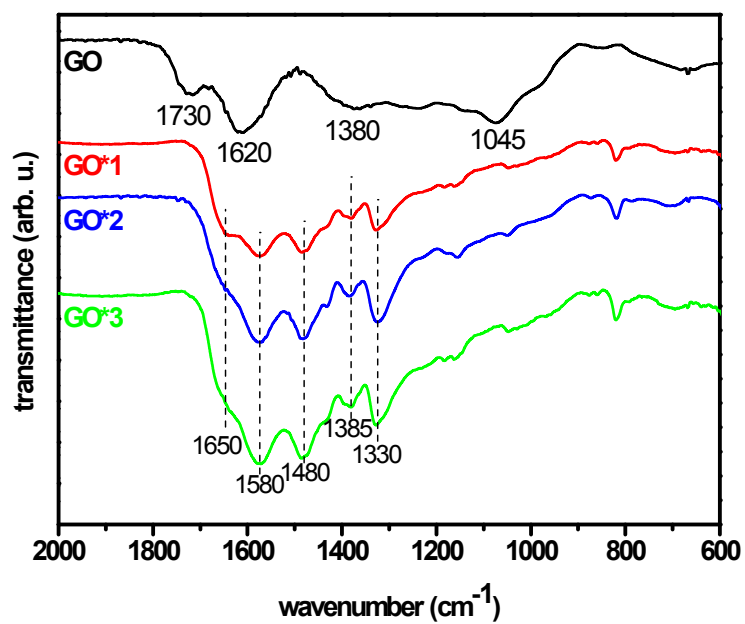


Fig. S1. FT-IR spectra of GO, GO*1, GO*2 and GO*3.

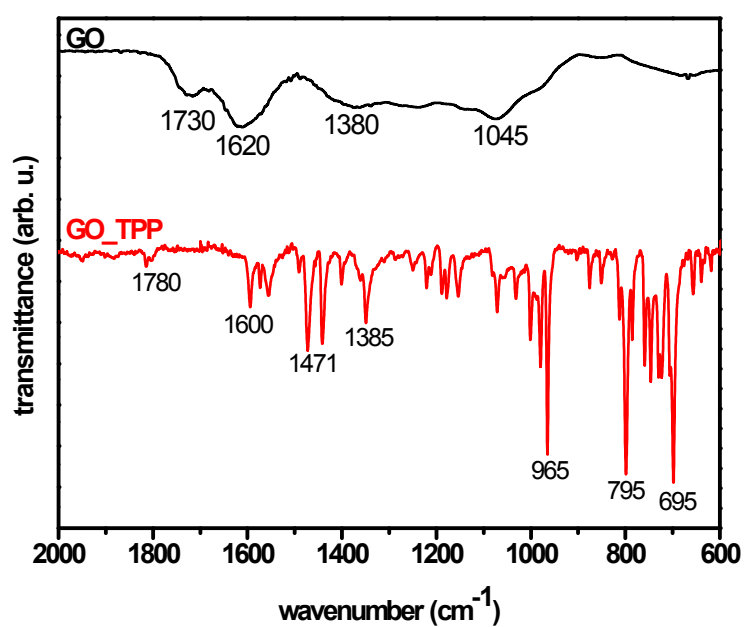


Fig. S2. Comparison between FT-IR spectra of GO and GO_TPP.

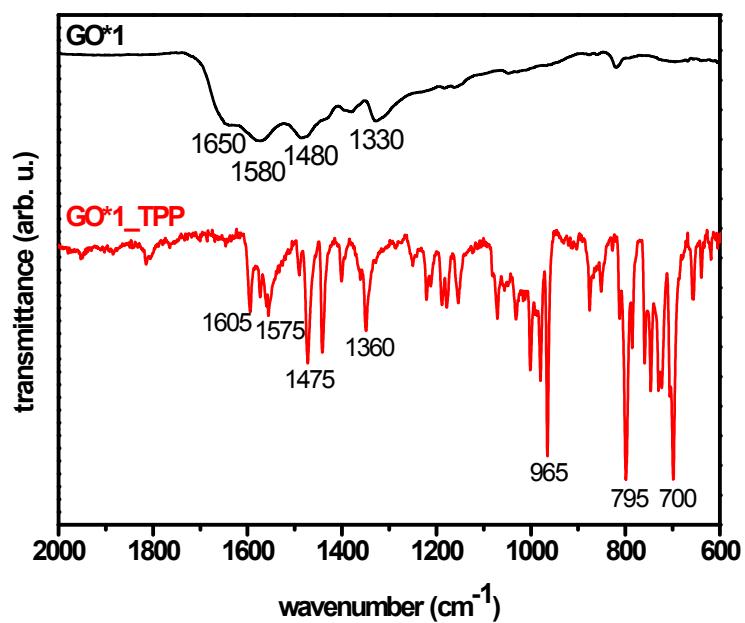


Fig. S3. Comparison between FT-IR spectra of **GO*1** and **GO*1_TPP**.

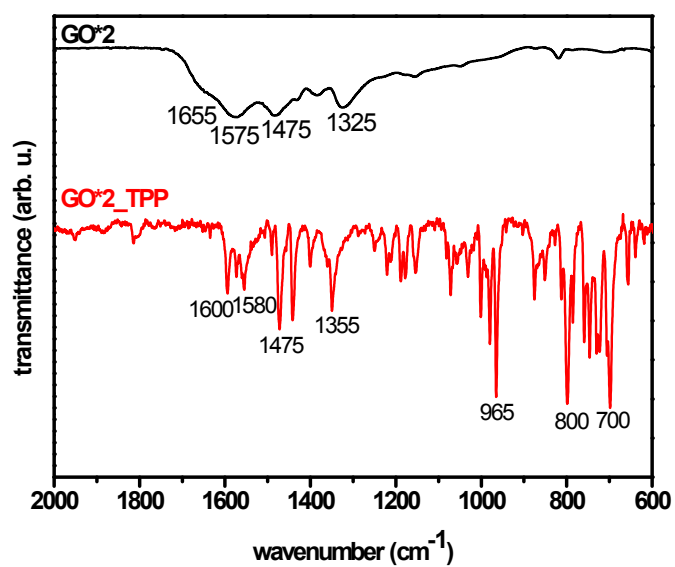


Fig. S4. Comparison between FT-IR spectra of **GO*2** and **GO*2_TPP**.

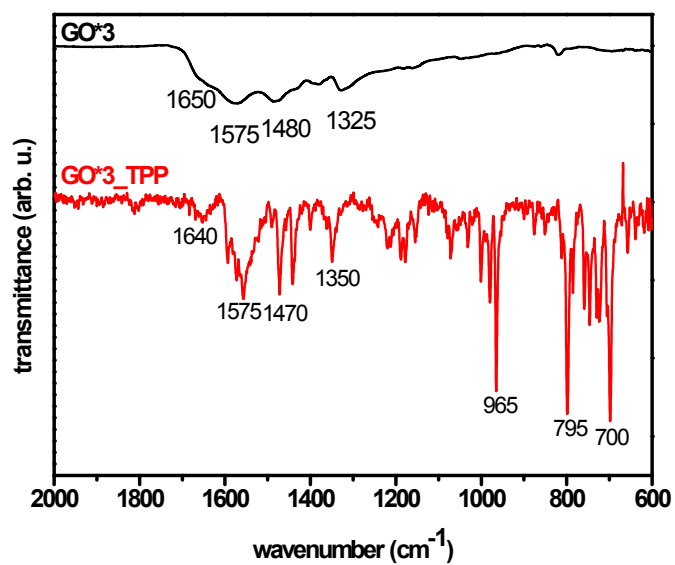


Fig. S5. Comparison between FT-IR spectra of GO*3 and GO*3_TPP.

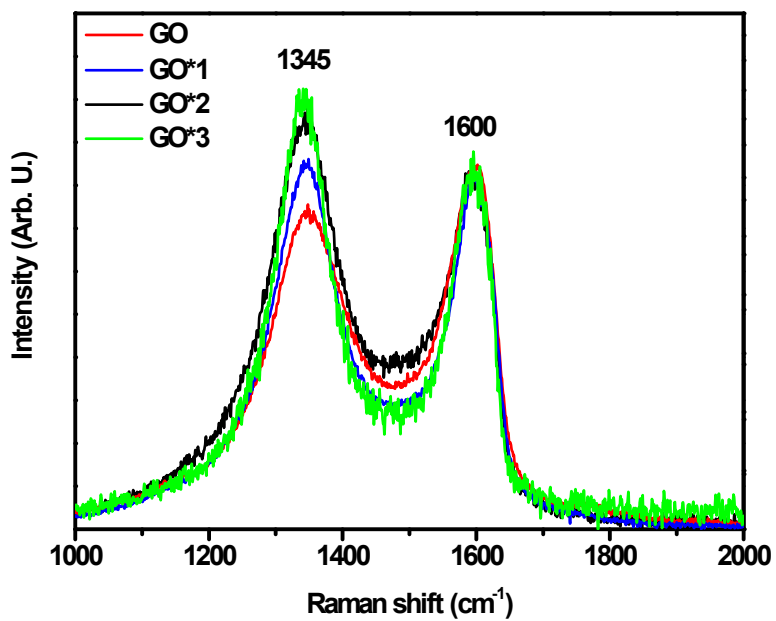


Fig. S6. Raman spectra of GO, GO*1, GO*2 and GO*3.

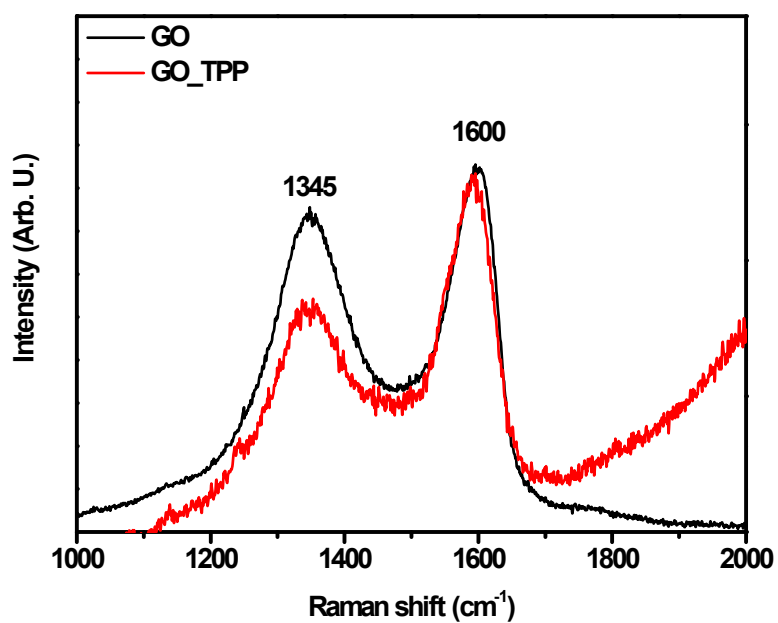


Fig. S7. Comparison between Raman spectra of GO and GO_TPP.

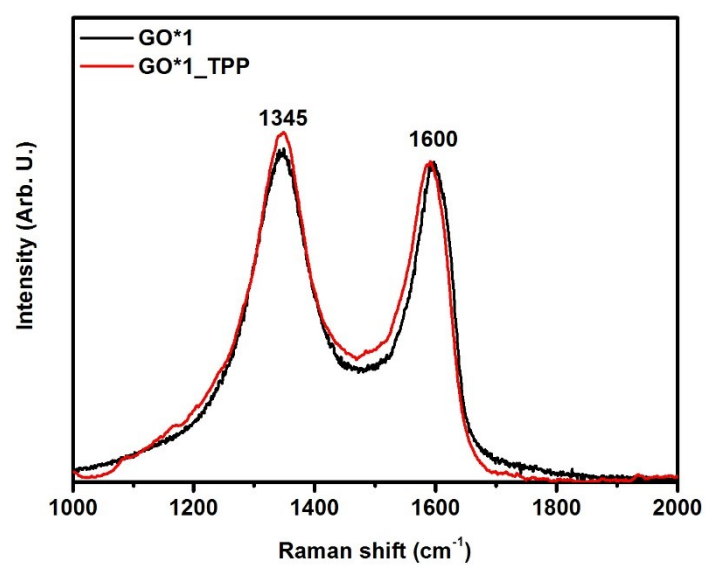


Fig. S8. Comparison between Raman spectra of GO*1 and GO*1_TPP.

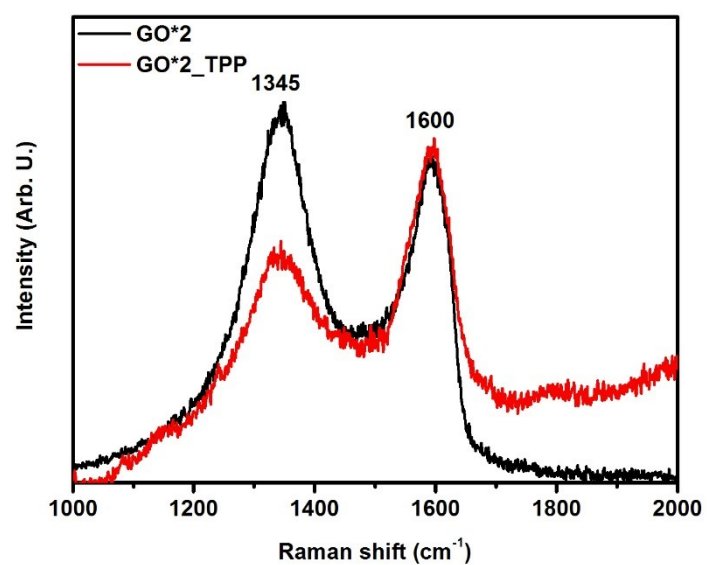


Fig. S9. Comparison between Raman spectra of **GO*2** and **GO*2_TPP**.

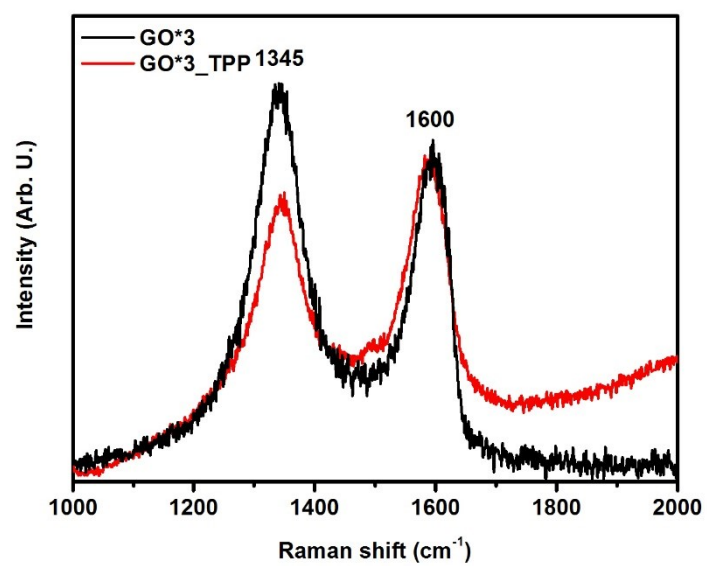


Fig. S10. Comparison between Raman spectra of **GO*3** and **GO*3_TPP**.

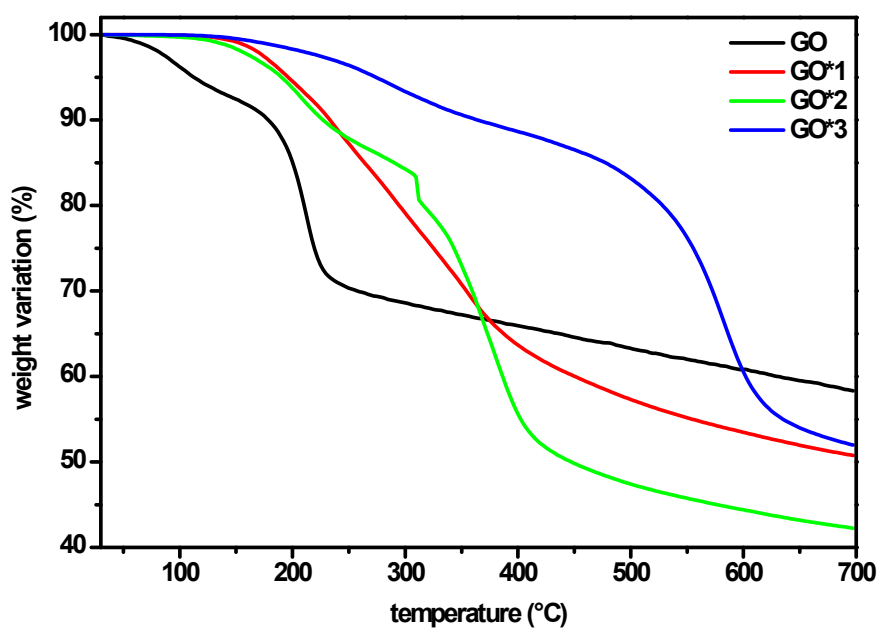


Fig. S11. TGA curves (argon atmosphere) of GO, GO*1, GO*2 and GO*3.

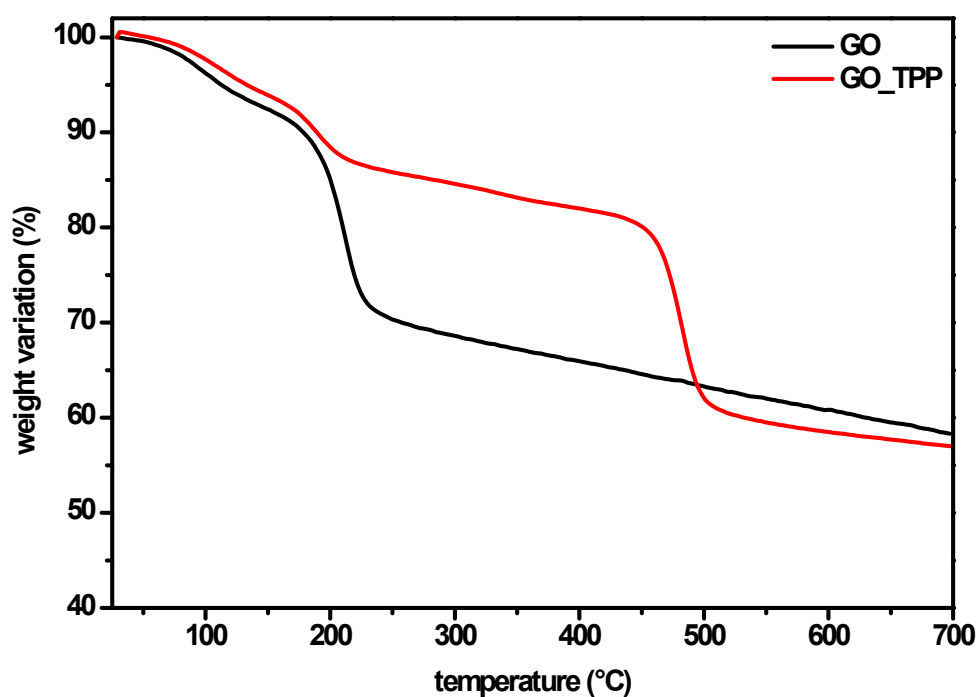


Fig. S12. Comparison between TGA curves (argon atmosphere) of GO and GO_TPP.

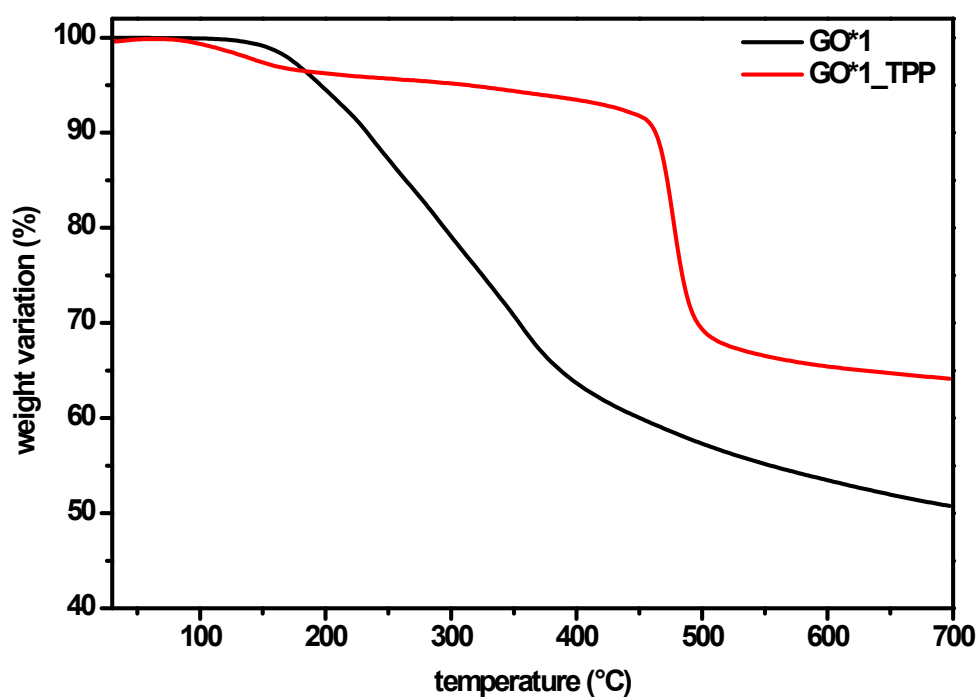


Fig. S13. Comparison between TGA curves (argon atmosphere) of GO*1 and GO*1_TPP.

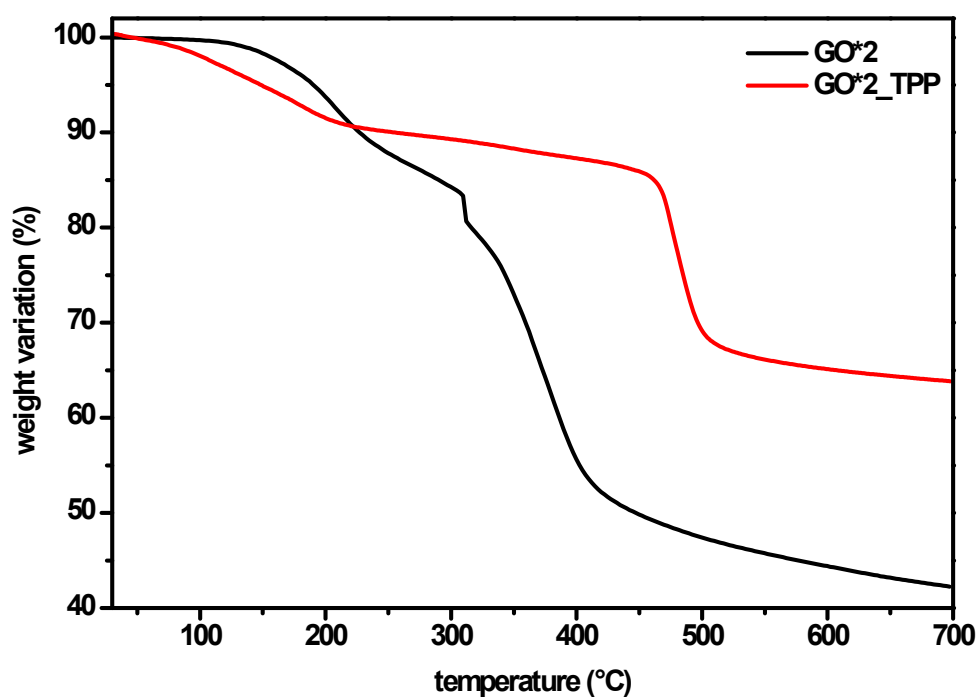


Fig. S14. Comparison between TGA curves (argon atmosphere) of GO*2 and GO*2_TPP.

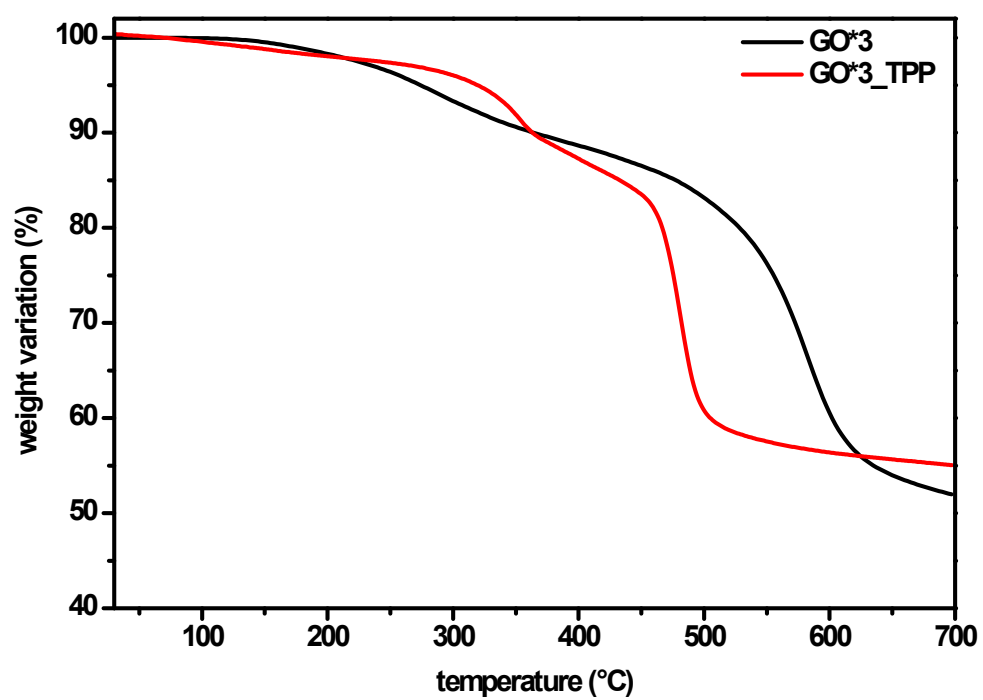
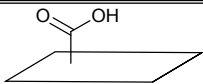
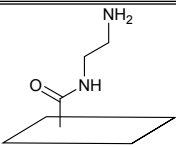
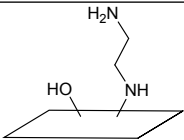
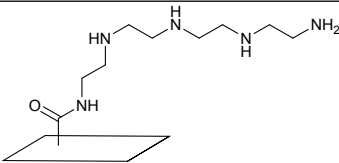
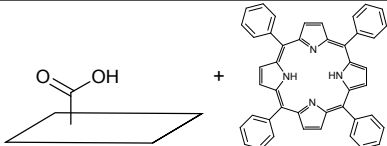
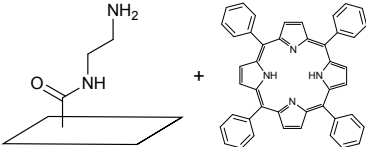
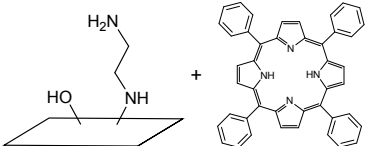
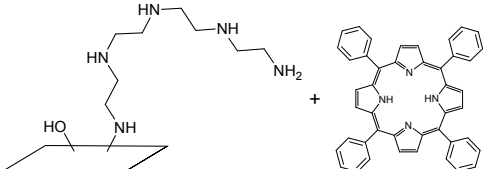


Fig. S15. Comparison between TGA curves (argon atmosphere) of **GO*3** and **GO*3_TPP**.

Table S1. Results of the elemental analysis for GO, **GO*1**, **GO*2** and **GO*3**.

Entry	Material label	Material structure	Elemental analysis data		
			%N	%C	%H
1	GO		-	47,57	2,67
2	GO*1		15,32	48,08	5,20
3	GO*2		11,32	50,45	4,14
4	GO*3		9,54	66,96	4,45
5	GO_TPP		4,60	54,46	3,64
6	GO*1_TPP		7,60	65,04	4,04
7	GO*2_TPP		7,04	57,74	3,99
8	GO*3_TPP		8,12	74,64	4,57

S4. Microbiological purity of GO

The microbiological analysis showed that GO was free from fungal and bacteria contaminations. After incubation of GO solutions on special substrates (48 h, 36°C) no colonies of microorganisms (fungal and bacteria) were observed (**Fig. S15**).

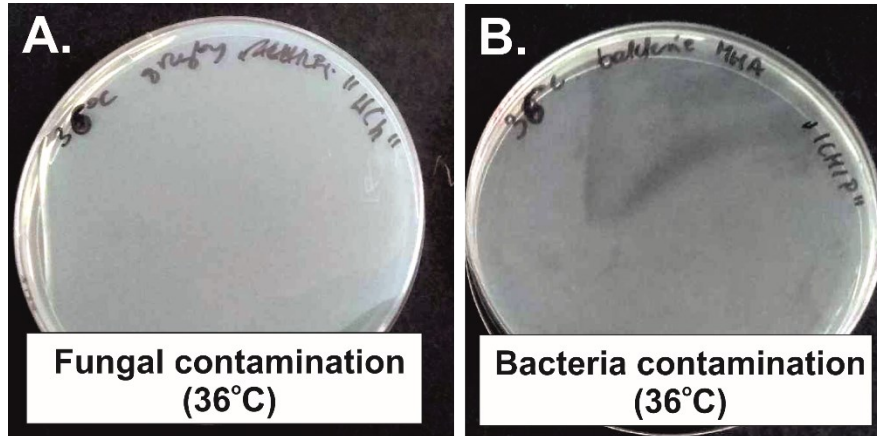


Fig. S16. *Results of microbial culture.*

S5. Fabrication of the microsystem

The microsystem was fabricated using the double casting technique. This method employs two forms: primary, which has the same structure as the final microsystem, and secondary, which is the negative of the final microsystem pattern. The primary form that contains a network of microchannels and microchambers, was fabricated with poly(methyl methacrylate) (PMMA) using a micromilling machine. Non-crosslinked PDMS (mixed prepolymer and crosslinking agent in a 9:1 weight ratio) was poured onto the primary form and allowed to cross-link (75°C, 1.5 h). Then, the form was separated from the PDMS block to obtain a secondary form with convex microstructures. The secondary form was subjected to the thermal aging (100°C, 48 h). After this time, the PDMS liquid crosslinking process was repeated on an aged form. The secondary form was separated from the crosslinked PDMS block and the bottom plate of the microsystem was obtained. The top plate of the microsystem was made by pouring liquid PDMS onto a flat glass plate. The crosslinked flat polymer plate was frozen in liquid nitrogen

and then holes for tubings were drilled. Both parts of the microsystem were degreased with detergent, washed with distilled water and dried with compressed air. Finally, the both plates were connected using an oxygen plasma.

S6. Photodynamic effect of GO_TPP *in vitro*

MCF-7 and HMF mono- cells cultures were subjected to the PDT procedure with different concentrations of GO_TPP ($10\div 100\ \mu\text{g mL}^{-1}$). After that, the effect of GO on cell viability was evaluated using the alamarBlue® assay. HMF cells were resistant to all the GO_TPP concentrations. In all cases, HMF were resistant to PDT procedure (HMF cells viability was about $90\% \pm 5\%$). However, MCF-7 cells showed a GO_TPP dose-dependent decrease in cell viability (**Fig. S17**). 24 h after PDT, MCF-7 viability for each GO_TPP derivative at highest concentration ($100\ \mu\text{g mL}^{-1}$ was about 45%).

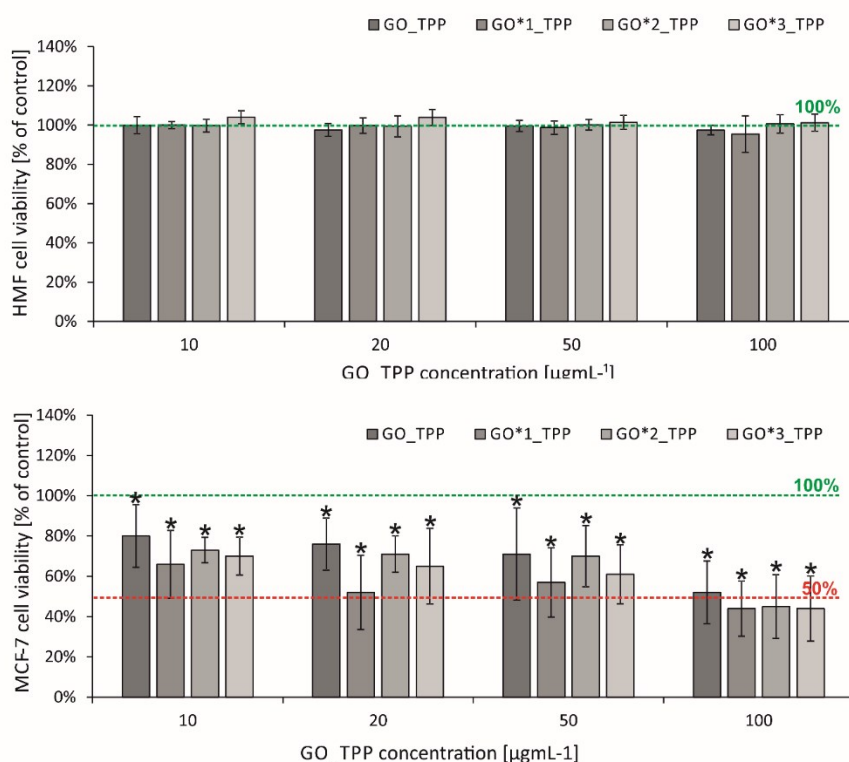


Fig. S17. The MCF-7 and HMF mono- cell cultures viability cultured as a monolayer in multi well-plates after PDT ($n = 3$, stars indicate $p < 0.05$).

References:

- [1] SDBSWeb: <https://Sdbs.Db.Aist.Go.Jp> (National Institute of Advanced Industrial Science and Technology, Date of Access – 29.08.2019).